JOURNAL OF COMPUTATIONAL PHYSICS 18, 165–187 (1975)

Simulation of Collisional Effects in Plasmas

C. E. RATHMANN AND J. DENAVIT

Department of Mechanical Engineering and Astronautical Sciences, Northwestern University, Evanston, Illinois 60201

Received November 25, 1974

A computer simulation method has been developed to simulate collisional effects in plasmas in the regime where plasma instabilities are dominant but are modified by weak collisions. The algorithm is based on the method of periodic smoothing in phase space, in which collisions are introduced at reconstruction times in terms of a one-dimensional Fokker–Planck operator with a velocity dependent collision frequency. The results of test problems, including approach to equilibrium, collisional heating, and plasma echo decay, are presented.

I. INTRODUCTION

Computer simulations of collisionless plasmas, based either on numerical solutions of the Vlasov equation or on equivalent particle simulation techniques, have been applied in recent years to studies of nonlinear oscillations, instabilities, and turbulent heating of plasmas. In a number of problems of interest in controlled thermonuclear fusion research and in space physics, weak collisional effects with collision frequencies of the order of a few percent of the plasma frequency may play a significant role in the development of instabilities and affect the turbulent state reached by the plasma after saturation.

In the anomalous absorption of radiation by plasmas, for example, the energy of the incoming radiation is first converted into plasma waves by parametric instabilities and the plasma waves in turn accelerate electrons by Landau damping, thus converting the wave energy into particle kinetic energy [1]. It is found, however, that in the case of collisionless plasmas, the absorbed energy appears in the form of suprathermal tails of the electron distribution function, rather than in the more desirable heating of the main body of the distribution function. A one-dimensional computer simulation method has been developed to study the weak collisional regime, in which the plasma oscillations and instabilities characteristic of collisionless plasmas remain dominant but are modified by collisions causing relaxations of the distribution function not present in the collisionless case. This method has been applied to the above anomalous absorption problem and the

results of this study, to be published separately [2], show that weak collisions can indeed channel a significant fraction of the absorbed energy into main body heating rather than in the formation of suprathermal tails.

The purpose of this paper is to describe the collision model used in this simulation method, together with its numerical implementation, and to present the results of a series of tests used to verify the validity of this approach.

The computations are one-dimensional, with spatial variations in the x direction, and only electrostatic fields are considered. In this paper we consider a single species representing electrons with the ions assumed stationary and providing only a charge neutralizing background. A version of the code including two species (electrons and ions) has been written and applied to the above study of parametric heating, but this generalization is straightforward and need not be discussed in detail. The algorithm is based on the method of periodic smoothing in phase space [3]. In this method, the phase space, which reduces to the (x, v) plane in the present case, is covered with a rectangular grid, Fig. 1, and weighted

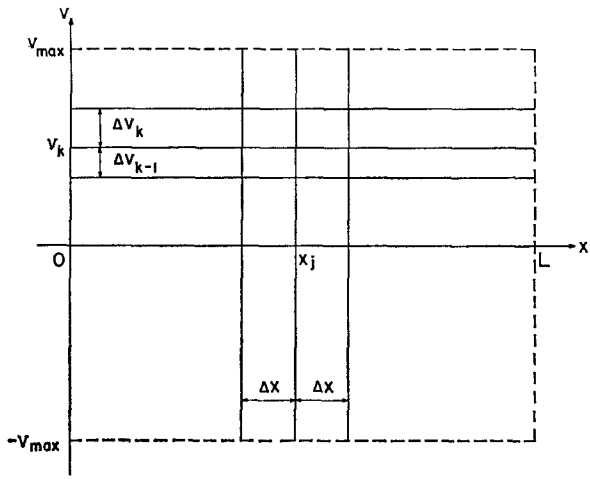

FIG. 1. Grid structure in x, v plane used for periodic reconstruction of distribution function.

simulation particles are initially located at each grid point with a mass (and charge) proportional to the local number of electrons in phase space. These particles are then advanced according to their self- and externally applied fields for $N = 5$ to 20 time steps, as in conventional particle simulation methods, after which the distribution function is reconstructed in phase space. The reconstruction, in effect, redistributes each simulation particle locally among neighboring grid points and the new particles are then advanced another N time steps. This procedure, which is equivalent to a numerical solution of the Vlasov equation, has

been found to be effective for reducing or eliminating the noise due to individual interactions of the simulation particles.

Electron-ion collisions are introduced into the computations in terms of the one-dimensional collision operator

$$\left(\frac{\partial f}{\partial t}\right)_{\text{coll}} = \frac{\partial}{\partial v}\left[\nu v f + D\frac{\partial}{\partial v}(\nu f)\right], \tag{1}$$

which is inserted in the right member of the Vlasov equation. The collision frequency ν may be velocity dependent, thus allowing a dependence of the form $\nu \sim v^{-3}$ corresponding to Coulomb collisions and D is a parameter to be specified by energy considerations. This operator conserves particles and its relationship with the Fokker–Planck operator is discussed in Appendix A. The first term in Eq. (1) accounts for a velocity-dependent friction force due to collisions, which tends to slow the particles, thereby reducing the kinetic energy. The second term accounts for a diffusion of particles in velocity space which leads to an increase in kinetic energy. Energy conservation may therefore be achieved by proper choice of the parameter D, given by

$$D = \int \nu v^2 f\, dv \Big/ \int \nu f\, dv, \tag{2}$$

as shown in Appendix A. Note that for a collision frequency independent of velocity, this value D reduces to the mean square velocity.

This model has been used in an analysis of collisional damping of plasma oscillations by Lenard and Bernstein [4] and in analytical and numerical studies of collisional effects on Landau damping by Zakharov and Karpman [5] and by Denavit, Doyle and Hirsch [6]. Collisional models of the same form, and with higher-order derivatives, have also been introduced in numerical solutions of the Vlasov equation using the Fourier–Hermite transform [7]. A collision frequency independent of velocity was assumed in these studies.

Numerical solutions of the three-dimensional Fokker–Planck equation have been carried out by Killeen and Marx [8]. This approach allows a much more realistic representation of the collisions than the simple one-dimensional model proposed in the present study, but at the cost of more complex computations. These solutions were concerned primarily with collisional effects and do not include the dynamics of plasma oscillations and instabilities, which remain the dominant aspects of the computations considered in the present paper. Computer simulations which include self-field dynamics as well as collisional effects have been done by Gula and Chu [9]. These simulations were based on the Krook collision model and were concerned with the effect of collisions on the evolution of the two-stream instability. In the Krook model the distribution function relaxes to a local Maxwellian distribution function at a rate which is independent of its

gradient in velocity space, while the collision operator defined by Eq. (1) includes derivatives which account for diffusion in velocity. This velocity diffusion is important in some problems such as in the collisional damping of plasma wave echoes, or in the evolution of the distribution function of resonant electrons resulting from Landau damping of plasma waves. Particle simulation methods can also be adapted to account for collisions by periodically adding a random increment to the velocity of each simulation particle, thereby causing these particles to perform a random walk in velocity space superimposed over their acceleration due to the self-consistent electric field. Such simulations have been carried out by Dawson and Shanny [10] and have more recently been applied to the anomalous heating problem by DeGroot [11].

The application of the present method to the anomalous heating problem requires a wide velocity range, up to $v_{\max} \simeq 20 v_{\text{th}}$ where v_{th} is the thermal velocity, to include the suprathermal tails of the electron distribution function after saturation, together with a sufficiently fine grid spacing, $\Delta v \simeq 0.1 v_{\text{th}}$ to describe adequately the main body of the distribution function which lies near the center of the velocity range. To meet these requirements economically the distribution function is reconstructed over a nonuniform velocity grid defined by

$$\frac{v_k}{v_{\max}} = S[2(k-1)/(k_{\max}-1) - 1], \qquad k = 1,\ldots, k_{\max}, \tag{3}$$

where $S(y)$ is a "stretch function" chosen to yield the desired grid point spacing.

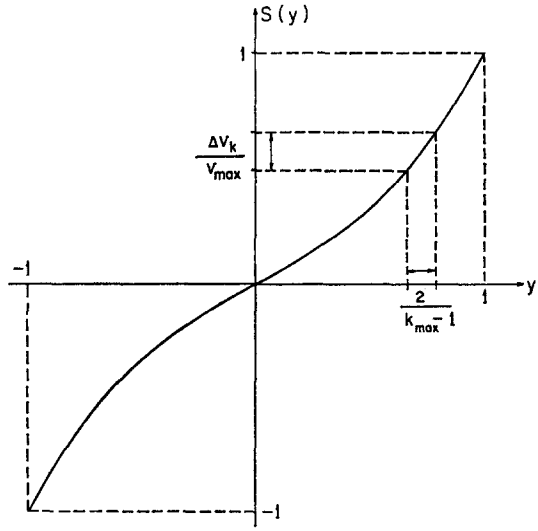

FIG. 2. Stretch function used to define nonuniform velocity grid.

For example, in the anomalous heating problem a stretch function given by

$$S(y) = \begin{cases} sy/(s+1-y) & \text{for} \quad 0 \leqslant y \leqslant 1, \\ sy/(s+1+y) & \text{for} \quad -1 \leqslant y \leqslant 0, \end{cases} \tag{4}$$

shown in Fig. 2 with $s = 1$, $v_{\max} = 20v_{\text{th}}$ and $k_{\max} = 63$, gives the desired fine spacing $\Delta v = v_{\text{th}}/6$ at $v = 0$ with a coarser spacing $\Delta v = 2v_{\text{th}}/3$ at $v = v_{\max}$.

The algorithm used in the computations is derived in Section II. A generalization of the reconstruction procedure for the distribution function over a nonuniform grid is considered first, after which the collision operator, Eq. (1), is introduced, considering the friction and diffusion terms separately. Since the application of the collision operator requires a knowledge of the distribution function, this operator is applied at reconstruction times, i.e., every 5 to 20 time steps, a procedure which is acceptable since only the weak collisional regime is considered in these computations. Between reconstructions, particles are advanced according to the ambient self- and externally applied electric fields as in collisionless simulations. Two series of tests have been carried out to verify the validity of this approach. The first series involves collisional effects in spatially uniform plasmas. These tests, presented in Section III, include approach to equilibrium and collisional heating due to constant and alternating electric fields. The second series, presented in Section IV, involves collisional effects on plasma oscillations and plasma echoes.

II. Development of the Algorithm

A. *Reconstruction of Distribution Function on Nonuniform Grid*

It has been shown [3] that by periodically reconstructing the distribution function within a particle code, the noise due to discrete particle interactions can be minimized. Such a reconstruction consists of a local averaging procedure in phase space, involving weight functions which determine what fraction of the mass of a given particle is assigned to each neighboring grid point. An averaging procedure which conserves mass, momentum, and energy has previously been derived for uniformly spaced grid points and this procedure is now generalized to the case of nonuniform grid spacing.

Consider the reconstruction of a given particle among its four nearest grid points in velocity, as illustrated in Fig. 3a. Let z denote the mass of the particle, let v_k denote the velocity associated with the grid point immediately below the particle, and let the grid points be separated by unequal increments as shown. The particle is located an amount $p\,\Delta v_k$ $(0 \leqslant p < 1)$ above grid point k. The first three moments are to be conserved in a symmetrical reconstruction among the four grid points. Accordingly, the particle is split into halves ($z^{(1)}$ and $z^{(2)}$)

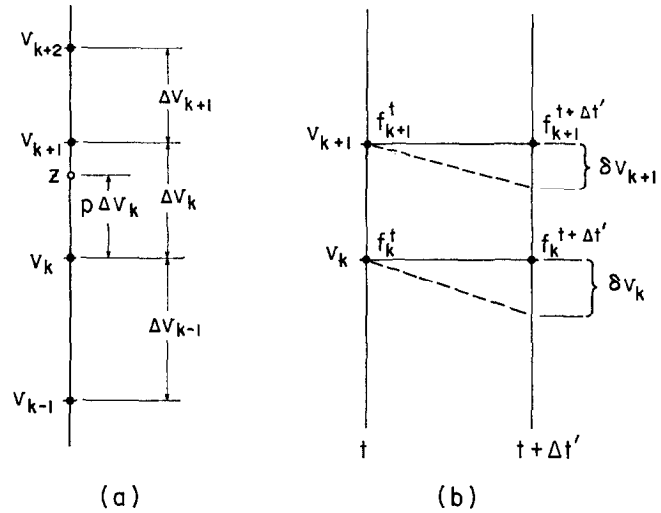

FIG. 3. (a) Redistribution of a particle z among four neighboring grid points. (b) Implementation of friction operator in terms of velocity increments δv_k.

and each half is distributed among three grid points so as to conserve the three moments independently. The contributions of the two halves are then added to determine the weight functions and to complete the averaging procedure. The first half, $z^{(1)} = z/2$, is replaced by the equivalent system $z_{k-1}^{(1)}$, $z_k^{(1)}$, $z_{k+1}^{(1)}$ at grid points $k-1$, k, and $k+1$ such that

$$(v_k - \Delta v_{k-1})^n z_{k-1}^{(1)} + v_k{}^n z_k^{(1)} + (v_k + \Delta v_k)^n z_{k+1}^{(1)} = (v_k + p\,\Delta v_k)^n (z/2), \qquad n = 0, 1, 2, \tag{5}$$

and $z^{(2)} = z/2$ is similarly replaced by the system $z_k^{(2)}$, $z_{k+1}^{(2)}$, $z_{k+2}^{(2)}$,

$$v_k{}^n z_k^{(2)} + (v_k + \Delta v_k)^n z_{k+1}^{(2)} + (v_k + \Delta v_k + \Delta v_{k+1})^n z_{k+2}^{(2)} = (v_k + p\,\Delta v)^n (z/2), \qquad n = 0, 1, 2. \tag{6}$$

Solving these sets of equations for the fractional masses $z_k^{(i)}$ and reassembling the particle halves yields the averaging procedure

$$\begin{aligned} z_{k-1} &= \left\{ \frac{p(p-1)}{2} \Big/ \left[\frac{\Delta v_{k-1}}{\Delta v_k} \left(\frac{\Delta v_{k-1}}{\Delta v_k} + 1 \right) \right] \right\} z, \\ z_{k+1} &= \left\{ p + \frac{p(p-1)}{2} \left[\frac{\Delta v_{k+1} - \Delta v_k - \Delta v_{k-1}}{\Delta v_{k+1}(\Delta v_{k-1} + \Delta v_k)} \Delta v_k \right] \right\} z, \\ z_{k+2} &= \left\{ \frac{p(p-1)}{2} \Big/ \left[\frac{\Delta v_{k+1}}{\Delta v_k} \left(\frac{\Delta v_{k+1}}{\Delta v_k} + 1 \right) \right] \right\} z, \\ z_k &= z - z_{k-1} - z_{k+1} - z_{k+2}. \end{aligned} \tag{7}$$

This averaging is sequentially applied to all simulation particles to generate the reconstructed distribution function. Weights assigned to velocities beyond the maximum velocity of the grid are neglected. However, the maximum velocity must be chosen sufficiently large to prevent any significant loss of particles. Note that the quantities in square brackets depend on the grid spacing only and therefore need to be computed only once, and that for uniform spacing, $\Delta v_{k-1} = \Delta v_k = \Delta v_{k+1}$, this averaging procedure reduces to the case considered earlier.

As in the case of a uniform grid spacing [3] the weights z_{k-1} and z_{k+2} are always negative and may yield unphysical oscillations or negative values of the distribution function where sharp changes occur over a few grid points. This effect is analogous to the appearance of small wiggles of wave number k_c in a function reconstructed from its Fourier transform in which wave numbers larger than k_c have been neglected. These wiggles can usually be controlled by assigning a sufficient number of grid points to regions of phase space where the distribution function has large gradients.

B. *Collision Operator*

The friction term in Eq. (1),

$$\left(\frac{\partial f}{\partial t}\right)_{\text{fric}} = \frac{\partial}{\partial v}\,[v\nu(v)\,f(v,\,t)],$$

is equivalent to the introduction of a velocity dependent acceleration $a(v) = -v\nu(v)$ into the equation of motion of the particles. The appropriate forms of the collision frequency $\nu(v)$ used in the present one-dimensional model are discussed in Appendix A. Since weak collisional effects are considered here, the collision operator, including both friction and diffusion terms, is applied at reconstruction times only. The friction term is therefore implemented by giving to each particle of velocity v_k, which is a grid point value at that time, a velocity increment $\delta v_k = a(v_k)\,\Delta t'$ where $\Delta t' = N\,\Delta t$ is the time interval between reconstructions, as shown in Fig. 3b.

The diffusion term in Eq. (1),

$$\left(\frac{\partial f}{\partial t}\right)_{\text{diff}} = D\,\frac{\partial^2}{\partial v^2}\,(\nu f),$$

is represented by finite differences over the nonuniform velocity grid. Let z_k denote the particle weight at the grid point k, the distribution function at this point has a value $f_k = 2z_k/(\Delta v_{k-1} + \Delta v_k)$. The diffusion operator is implemented by giving to each value of the distribution function an increment

$$\delta f_k = \frac{\alpha}{\Delta v_{k-1} + \Delta v_k}\left\{\frac{(\nu f)_{k+1} - (\nu f)_k}{\Delta v_k} - \frac{(\nu f)_k - (\nu f)_{k-1}}{\Delta v_{k-1}}\right\},$$

where $\alpha = 2D\,\Delta t'$, or in terms of particle weights,

$$\delta z_k = \alpha \left\{ \frac{(\nu z)_{k+1}}{\Delta v_k(\Delta v_k + \Delta v_{k+1})} - \frac{(\nu z)_k}{\Delta v_{k-1}\,\Delta v_k} + \frac{(\nu z)_{k-1}}{\Delta v_{k-1}(\Delta v_{k-1} + \Delta v_{k-2})} \right\}. \quad (8)$$

This explicit procedure is numerically stable only if the coefficient of z_k in the right member of Eq. (8) has a magnitude less than or equal to unity, i.e.,

$$\frac{\alpha \nu_k}{\Delta v_{k-1}\,\Delta v_k} \leqslant 1 \quad (9)$$

If this condition is not satisfied, the coefficient α is divided by an integer l such that (9) is satisfied, and Eq. (8) is repeated l times, thus applying the diffusion operator as a sequence of l steps, each corresponding to a time interval $\Delta t'/l$.

III. Spatially Homogeneous Problems

The above algorithm is tested in this section by considering simple collisional problems in spatially homogeneous plasmas, where no internal electric fields are present.

A. *Approach to Equilibrium*

As a first example we consider the approach to equilibrium of two Maxwellian beams defined initially by the distribution function,

$$f(v, t = 0) = \frac{n}{2(2\pi)^{1/2} v_{b0}} \left\{ \exp\left[-\frac{1}{2}\left(\frac{v - v_{d0}}{v_{b0}} \right)^2 \right] + \exp\left[-\frac{1}{2}\left(\frac{v + v_{d0}}{v_{b0}} \right)^2 \right] \right\}, \quad (10)$$

where v_{b0} defines the initial thermal spread of each beam and $\pm v_{d0}$ defines their initial drifts relative to the origin of velocities. With no external field, the governing equation for the one-dimensional model is

$$\frac{\partial f}{\partial t} = \frac{\partial}{\partial v}\left[\nu v f + D \frac{\partial}{\partial v}(\nu f) \right]. \quad (11)$$

For a collision frequency ν independent of velocity, the coefficient D defined by Eq. (2) for energy conservation, is equal to the mean square velocity $\langle v^2 \rangle$ and remains constant, i.e., $D = 2(v_{b0}^2 + v_{d0}^2)$. In this case Eq. (11) with the initial distribution function (10) may be solved analytically by taking a Fourier transform with respect to velocity. This solution yields

$$f(v, t) = \frac{n}{2(2\pi)^{1/2} v_b} \left\{ \exp\left[-\frac{1}{2}\left(\frac{v - v_d}{v_b} \right)^2 \right] + \exp\left[-\frac{1}{2}\left(\frac{v + v_d}{v_b} \right)^2 \right] \right\} \quad (12)$$

where $v_b = [D - (D - v_{b0}^2)\exp(-2\nu t)]^{1/2}$ and $v_d = v_{d0}\exp(-\nu t)$. Thus the beams retain their Maxwellian form in this case but their drift decays due to friction while their thermal spread increases due to velocity diffusion. As $t \to \infty$ the beams merge into a single Maxwellian distribution function,

$$f(v, t \to \infty) = [n/(2\pi D)^{1/2}] \exp[-\tfrac{1}{2}(v^2/D)]. \tag{13}$$

The results of a numerical simulation of this problem are shown in Fig. 4. This

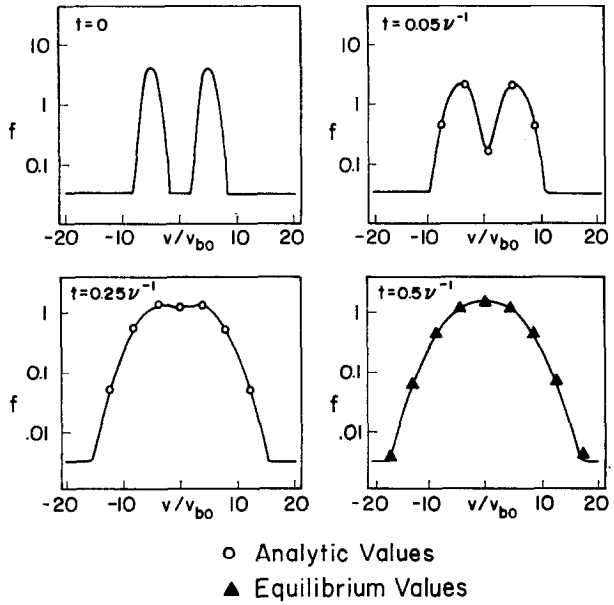

FIG. 4. Collision relaxation of a two-beam distribution function with ν constant and $v_{d0} = 5v_{b0}$.

case corresponds to $v_{d0} = 5v_{b0}$ with $v_{\max} = 20v_{b0}$ and a nonuniform grid spacing with 125 points and $s = 1$. The time interval between reconstructions is $\Delta t' = 0.025\nu^{-1}$. The numerical results, shown in solid line, agree closely with the analytical values from Eq. (12) shown as circles. The distribution function at $t = 0.5\nu^{-1}$ reaches a form close to its equilibrium defined by Eq. (13), which appears as a parabola on the logarithmic plot of Fig. 4.

We now consider a velocity-dependent collision frequency of the form

$$\nu = C/(2\langle v^2\rangle + v^2)^{3/2}, \tag{14}$$

appropriate for a one-dimensional representation of Coulomb collisions, as

discussed in Appendix A, where $\langle v^2 \rangle$ denotes the mean square velocity and C is a collisional constant. The coefficient D given by Eq. (2) becomes time dependent for this case and the equilibrium distribution function is not Maxwellian but takes the form

$$f(v, t \to \infty) = \frac{0.3537n}{\langle v^2 \rangle^{1/2}} \left(1 + \frac{v^2}{2\langle v^2 \rangle}\right)^{3/2} e^{-0.88v^2/\langle v^2 \rangle}. \tag{15}$$

This equilibrium distribution function is derived in Appendix B. For the present problem, where the mean square velocity remains constant, it is convenient to write $C = (3\langle v^2 \rangle)^{3/2} \nu_0$, where ν_0 may be interpreted as the collision frequency of a particle having a velocity equal to the thermal velocity.

The results of a numerical simulation for this case are shown in Fig. 5. The same parameters are used as in the simulation of Fig. 4 with $\Delta t' = 0.025\nu_0^{-1}$ and time measured in units of ν_0^{-1}. We observe that the approach to equilibrium is slower in the present case. The distribution function reaches a form close to its equilibrium for $t = 1.5\nu_0^{-1}$, instead of $t = 0.5\nu^{-1}$ for the case where ν is independent of velocity. The equilibrium distribution function defined by Eq. (15) is shown by the triangles on the diagram for $t = 1.5\nu_0^{-1}$. Note the flatter top and more steeply dropping tails of this equilibrium distribution function compared to the Maxwellian distribution at $t = 0.5\nu^{-1}$ in Fig. 4.

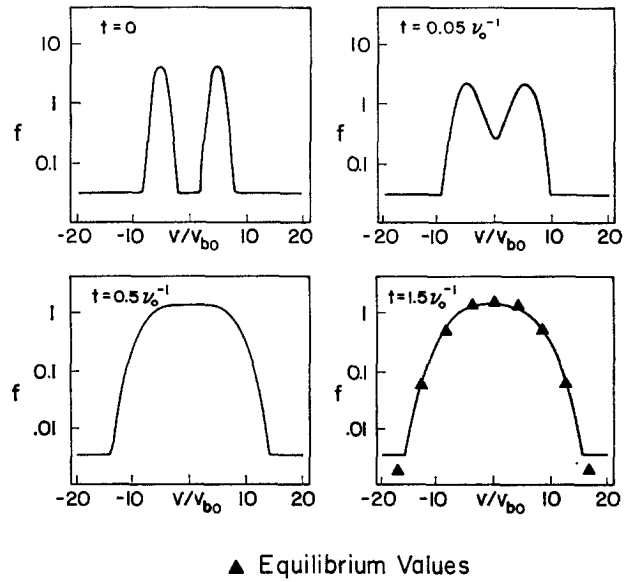

FIG. 5. Collisional relaxation of a two-beam distribution function with $\nu = (3/2)^{3/2}\nu_0(1 + v^2/2v_T^2)^{-3/2}$ and $v_{b0} = 5v_{b0}$.

The computations of Figs. 4 and 5 have been repeated with the same parameters but using a uniform grid spacing, and results very close to those of Figs. 4 and 5 were obtained.

B. *Collisional Heating*

As a second example we consider the heating of a homogeneous plasma by dc and ac external electric fields, governed by the equation

$$\frac{\partial f}{\partial t} - \frac{eE}{m}\frac{\partial f}{\partial v} = \frac{\partial}{\partial v}\left[vf + D\frac{\partial}{\partial v}(vf)\right], \tag{16}$$

with the initial distribution function

$$f(v, t = 0) = [n/(2\pi)^{1/2} v_{T_0}] \exp[-\tfrac{1}{2}(v/v_{T_0})^2]. \tag{17}$$

For a collision frequency independent of velocity, Eq. (16) may be integrated and yields

$$f(v, t) = [n/(2\pi)^{1/2} v_T] \exp\{-\tfrac{1}{2}[(v - v_d)/v_T]^2\}, \tag{18}$$

where

$$\frac{dv_d}{dt} + \nu v_d = -\frac{eE}{m}, \tag{19}$$

$$\frac{d}{dt} v_T^2 = 2\nu v_d^2. \tag{20}$$

For a dc electric field, Eq. (19) gives $v_d = -(eE/\nu m)[1 - \exp(-\nu t)]$. Thus the distribution function remains Maxwellian and after a transient of duration $\sim\nu^{-1}$ acquires a drift $v_d = -eE/\nu m$. The kinetic energy relative to the drift motion, $T = mn(\langle v^2\rangle - \langle v\rangle^2)/2$ then increases linearly according to Eq. (20) at a rate given by

$$\frac{d}{d(\omega_p t)}\left(\frac{T}{T_0}\right) = 2\frac{\omega_p}{\nu}\frac{U}{T_0}, \tag{21}$$

where $\omega_p = (4\pi e^2 n/m)^{1/2}$ is the plasma frequency, $T_0 = nmv_{T_0}^2/2$ is the initial kinetic energy density and $U = E^2/8\pi$ is the energy density of the applied field. The results of a computer simulation of this problem, with $\nu = 0.05\omega_p$ and $\eta^2 = U/T_0 = E^2/4\pi nmv_{T_0}^2 = 6.25 \times 10^{-4}$ are shown in Figs. 6a and 7. This simulation was carried out with $\Delta t = \Delta t' = 0.2\omega_p^{-1}$, $v_{\max} = 10v_{T_0}$ and a uniform grid with 63 points. We observe in Fig. 6a that the distribution function acquires a drift $v_d = -\omega_p \eta v_{T_0}/\nu = -0.5v_{T_0}$ after $t = 50\omega_p^{-1}$ and broadens while remaining Maxwellian. The kinetic energy ratio T/T_0 shown in Fig. 7 increases at the predicted rate after $t = 50\omega_p^{-1}$.

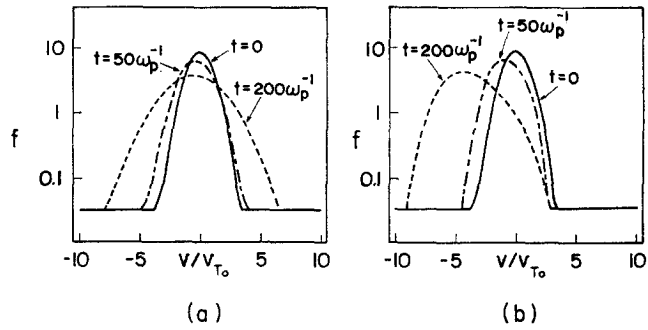

FIG. 6. Collisional heating by a dc electric field, $\eta^2 = U/T_0 = 6.25 \times 10^{-4}$. (a) $\nu = 0.05\ \omega_p$ (constant); (b) $\nu = (3/2)^{3/2}\nu_0(v_{T_0}/v_T)^3(1 + v^2/2v_T^2)^{-3/2}$ with $\nu_0 = 0.05\ \omega_p$.

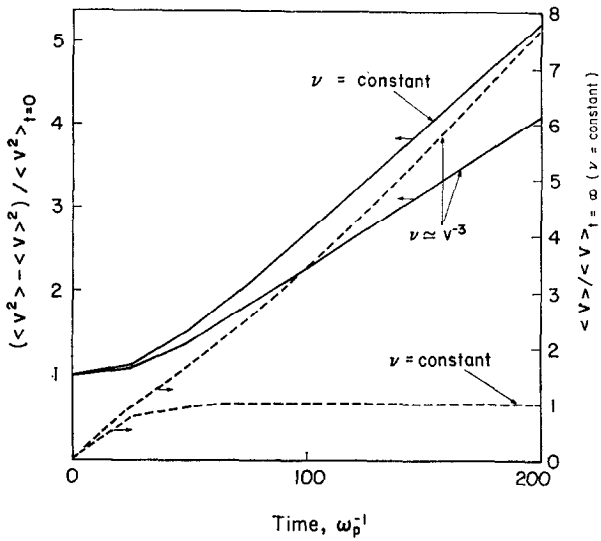

FIG. 7. Increase in random motion kinetic energy (solid lines) and in momentum (broken lines) under a dc field, $\eta^2 = 6.25 \times 10^{-4}$, for $\nu = 0.05\ \omega_p$ (constant) and for $\nu = (3/2)^{3/2}\nu_0$ $(v_{T_0}/v_T)^3(1 + v^2/2v_T^2)^{-3/2}$ with $\nu_0 = 0.05\ \omega_p$.

For an ac electric field $E = E_0 \cos \omega_0 t$, Eq. (19) gives an oscillating drift velocity

$$v_d = -[\omega_p\eta/(\nu^2 + \omega_0^2)][\omega_0 \sin \omega_0 t + \nu \cos \omega_0 t]\, v_{T_0},$$

after a transient of duration $\sim\nu^{-1}$. The kinetic energy density, averaged over a period $2\pi/\omega_0$, increases linearly at a rate given by

$$d(\langle T\rangle/T_0)/d(\omega_p t) = \nu\omega_p\eta^2/(\nu^2 + \omega_0^2), \tag{22}$$

where $\eta^2 = E_0^2/4\pi nmv_{T_0}^2$. A computer simulation was carried out for this case with $\nu = 0.05\omega_p$, $\omega_0 = 1.04\omega_p$, $\eta^2 = 0.25$, and the same finite differences as in the dc case. The distribution function, shown in Fig. 8a, broadens but remains Maxwellian and the average kinetic energy density, shown in Fig. 9, increases linearly at the rate predicted by Eq. (22). The deviation from the linearly increasing energy evident for $t > 360\omega_p^{-1}$ is due to loss of particles over the edges of the velocity grid at $\pm v_{\max}$.

In the case of a velocity-dependent collision frequency of the form given by

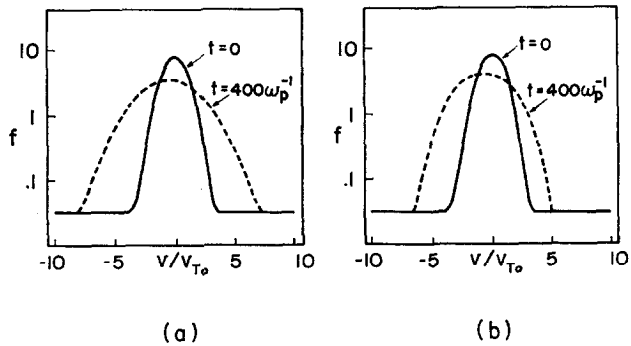

FIG. 8. Collisional heating by an ac electric field, $\eta^2 = U/T_0 = 0.25$, $\omega_0 = 1.04\,\omega_p$. (a) $\nu = 0.05\,\omega_p$ (constant); (b) $\nu = (3/2)^{3/2}\nu_0(v_{T_0}/v_T)^3(1 + v^2/2v_T^2)^{-3/2}$ with $\nu_0 = 0.2\,\omega_p$.

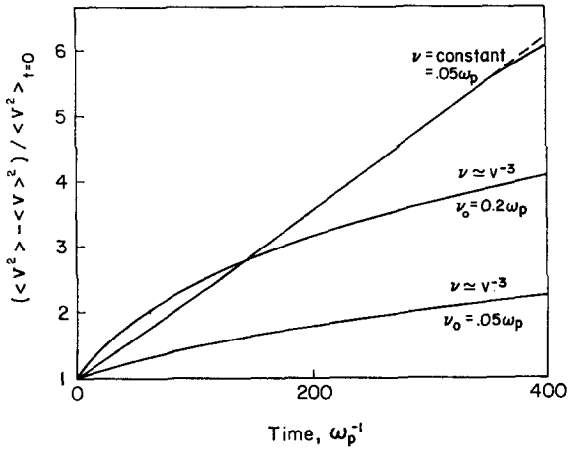

FIG. 9. Increase in random motion kinetic energy under an ac field, $\eta^2 = 0.25$, $\omega_0 = 1.04\,\omega_p$, $\nu = 0.05\,\omega_p$ (constant) and $\nu = (3/2)^{3/2}\nu_0(v_{T_0}/v_T)^3(1 + v^2/2v_T^2)^{-3/2}$ with $\nu_0 = 0.05\,\omega_p$ and $\nu_0 = 0.2\,\omega_p$. The broken line represents the theoretically predicted linear increase.

Eq. (14), a simple exact integration of Eq. (16) does not appear to be possible. The external field causes a drift velocity $\langle v \rangle$ given by the first moment of Eq. (16),

$$\frac{\partial \langle v \rangle}{\partial t} + \frac{1}{n} \int_{-\infty}^{+\infty} \nu v f \, dv = -\frac{eE}{m}, \tag{23}$$

and the rate of increase of the kinetic energy density is

$$\frac{mn}{2} \frac{\partial}{\partial t} \langle v^2 \rangle = -eEn\langle v \rangle. \tag{24}$$

However, when ν is velocity dependent, the distribution function cannot be eliminated from the integral in Eq. (23) and the system of Eqs. (23) and (24) cannot be solved.

Computer simulations of this problem have been carried out for dc and ac external fields. The results for the dc case, with $\nu_0 = 0.05\omega_p$ and the same initial distribution and parameters as in the case where ν is independent of velocity, are shown in Figs. 6b and 7. We observe in Fig. 6b that the distribution function acquires a drift and broadens, but does not remain Maxwellian. The drift velocity, which is shown in broken line in Fig. 7, increases steadily in the present case. The drift velocity results from a competition between the electric field and the friction force, and a steady drift velocity is achieved when the friction force balances the electric field. In the $\nu =$ constant case this balance occurs after a transient of duration $\sim\nu^{-1}$, as shown in Fig. 7, after which only heating takes place. In the present case, however, the increase in the mean square velocity $\langle v^2 \rangle$ due to both drift and heating reduces the collision frequency (see Eq. (14)), and a balance between the electric field and the friction force cannot be achieved.

In the case of an ac external field, the runaway effect described above does not occur, but the heating is expected to cause a reduction in the collision frequency, resulting in a decreasing heating rate proportional to $(T/T_0)^{-3/2}$. The results of a computer simulation in this case are shown in Figs. 8b and 9. This computation was carried out with $\nu_0 = 0.2\omega_p$, larger than the value assumed in previous computations, but with the same initial distribution and parameters as in the $\nu =$ constant case. We note in Fig. 8b that the distribution function broadens but does not remain Maxwellian. The kinetic energy ratio T/T_0 shown in Fig. 9 increases at a rate which is proportional to $(T/T_0)^{-3/2}$ as expected. The kinetic energy ratio for an additional computation with $\nu_0 = 0.05\omega_p$ is also shown in Fig. 9. We observe that the heating rate for this case is less than that for a constant collision frequency having the same value, $\nu = 0.05\omega_p$.

IV. Collisional Damping of Plasma Wave Echoes

The simulation method is now tested by considering the collisional damping of second-order temporal plasma wave echoes. A uniform stable plasma is initially excited by an external longitudinal electric field pulse with wave number k_1. This mode decays at the Landau damping rate γ_1 and, in the collisionless case, the distribution function acquires a perturbation of the form $f_1(v) \exp(-ik_1x + ik_1vt)$. For large t the integral over v of this perturbation phase mixes and does not result in any density or field perturbation. A second wave of wave number k_2 is then excited by a pulse at time $\tau \gg 1/\gamma_1$. This wave also damps out, but modulates the distribution function of the first wave to give a second-order distribution function of the form $f_1(v) f_2(v) \exp[ik_3x - ik_3v(t - k_2\tau/k_3)]$ of wave number $k_3 = k_2 - k_1$. At time $\tau' = k_2\tau/k_3$ the coefficient of v in this exponential vanishes and the integral over v no longer phase mixes. A new wave of wave number k_3, called an echo, then appears in the plasma. Since perturbations of the form $\exp(ikvt)$ are strongly affected for large t by the velocity diffusion term of the collision operator, Eq. (1), the plasma echo appears as a useful test of the present algorithm for small values of the collision frequency.

Plasma wave echoes in collisionless plasmas have been treated theoretically by O'Neil and Gould [12], and the effect of collisions in the damping of echo waves has been examined by Su and Oberman [13], O'Neil [14], and Ichikawa and Suzuki [15] using collisional operators of the same form as Eq. (1). Computer simulations of plasma wave echoes, including collisional effects, have been made by Brackbill [16] using a distribution pushing algorithm.

For second-order temporal echoes, the analytical results may be written in the form

$$\frac{E_3^{\text{echo}}(t)}{(4\pi nm)^{1/2}\, v_T} = \frac{\eta_1\eta_2}{4} \int_{-\infty}^{+\infty} \frac{e^{ik_1v\tau - \Lambda(t)}}{\epsilon(-k_1, ik_1v)} \frac{\partial f_0}{\partial (v/v_T)} \times \frac{\partial}{\partial s} \left[\frac{e^{s(t-\tau)}}{\epsilon(k_2, s - ik_1v)\, \epsilon(k_3, s)} \right]_{s=-ik_3v} dv, \tag{25}$$

where $\eta_1 = eE_1^{\text{ext}}\, \delta t_1/mv_T$, $\eta_2 = eE_2^{\text{ext}}\, \delta t_2/mv_T$, E_1^{ext} and E_2^{ext} are the electric fields of the first and second pulses, δt_1 and δt_2 their durations, $E_3^{\text{echo}}(t)$ is the echo electric field, $v_T = \langle v^2 \rangle^{1/2}$,

$$\epsilon(k, s) = 1 - \frac{i\omega_p^2}{k} \int_{-\infty}^{+\infty} \frac{\partial f_0/\partial v}{s + ikv}\, dv$$

is the dielectric function of the plasma, and f_0 is the unperturbed distribution

function. The quantity $\Lambda(t)$ which accounts for the collisions has been given by O'Neil as

$$\Lambda_O = \int_0^\tau \nu D k_1^2 t'^2 \, dt' + \int_\tau^t \nu D[-k_3(t' - \tau) + k_1\tau]^2 \, dt'$$

$$= \frac{\nu D}{3} \{k_1^2\tau^3 + k_3^2[(t - \tau')^3 - (\tau - \tau')^3]\}, \tag{26}$$

while the expression derived by Ichikawa and Suzuki is

$$\Lambda_{I-S} = \frac{\nu D}{3} [k_1^2\tau^3 + k_3^2(t - \tau)^3 + 3k_3^2\tau(t - \tau)^2 - 3k_1k_3\tau^2(t - \tau)]. \tag{27}$$

In both expressions only the diffusion term in Eq. (1) has been considered because the friction term has a negligible effect for the small values of the collision frequency considered here.

Although these expressions agree at the peak of the echo, $t = \tau'$, they yield different values of the damping for the wings. $\Lambda_o(t)$ varies slowly near $t = \tau'$ and has symmetrical values for the rise ($t < \tau'$) and the decay ($t > \tau'$) of the echo, while $\Lambda_{I-S}(t)$ increases with time giving a larger damping for the decay than for the rise. It should be observed that certain approximations were made in deriving both expressions. The diffusion operator is applied only to the exponential terms $\exp(ikvt)$ in the derivation of Eq. (26). The velocity derivatives of the coefficient of $\exp(ikvt)$, which involves f_0, ϵ, and ν, are neglected and Λ_o is valid only for sufficiently long times. In the derivation of Eq. (27) an expansion is made which assumes $\Lambda_{I-S} \ll 1$ so that large values of the damping constant from Eq. (27) may not be reliable.

A set of computations has been carried out for a Maxwellian distribution function with $k_1\lambda_D = 0.7$, $k_2\lambda_D = 1.4$, $\tau = 20\omega_p^{-1}$, and $\eta_1 = \eta_2 = 0.08$. Note that the echo mode $k_3 = k_2 - k_1 = k_1$ is the same as the initial wave mode for this choice of k_1 and k_2. Three cases with $\nu = 0$ (collisionless), $\nu = 0.001\omega_p$ (velocity independent) and $\nu = (3/2)^{3/2}\nu_0(1 + v^2/2v_T^2)^{-3/2}$ with $\nu_0 = 0.004$ have been considered. These parameters correspond to Landau damping rates $\gamma_1 = -0.37\omega_p$ and $\gamma_2 = -1.6\omega_p$ for modes k_1 and k_2 respectively. These computations were made with a uniform velocity grid with $v_{\max} = 5v_T$, $\Delta v = 0.04v_T$, $\Delta x = 0.56\lambda_D$ and $\Delta t = 0.1\omega_p^{-1}$. The distribution function was reconstructed and the collision operator applied every 20 time steps.

The maxima of the ratio of electrostatic energy to kinetic energy, $U_1/T = |E_1|^2/4\pi nmv_T^2$, for mode $k_1 = k_3$ are plotted in Fig. 10 for the collisionless case and both collisional cases. In all three cases the initial wave decays at approximately the Landau damping rate and the collisions have no observable effect on the damping rate, as expected for such small collision frequencies. For $t \simeq 14\omega_p^{-1}$

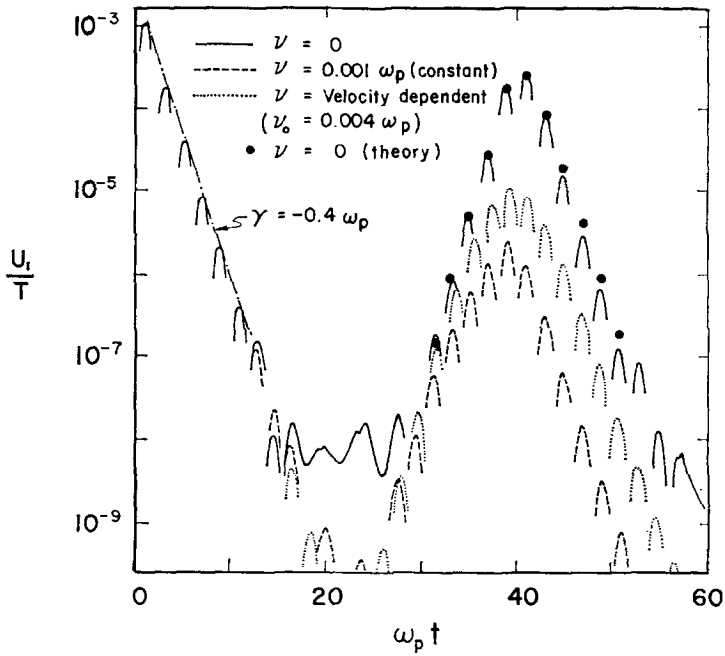

FIG. 10. Collisional damping of plasma wave echo with $k_1\lambda_D = 0.7$, $k_2\lambda_D = 1.4$, $\tau = 20\,\omega_p^{-1}$, $\eta_1 = \eta_2 = 0.08$. Collisional cases correspond to $\nu = 0.001\,\omega_p$ (constant) and $\nu = (3/2)^{3/2}\nu_0(1 + v^2/2v_T^2)^{-3/2}$ with $\nu_0 = 0.004\,\omega_p$.

the initial wave energy has decayed 5 orders of magnitude and the collisionless computations appear to have reached their noise level while in the collisional computations, which have a lower noise level, the energy continues to decay. For $t \gtrsim 27\omega_p^{-1}$ the echo wave appears, reaches its peak in all three cases near $\tau' = k_2\tau/k_3 = 40\omega_p^{-1}$ as expected and decays for $t > \tau'$. We observe, however, that the echo is significantly weaker in the collisional cases than in the collisionless case.

Values of the maxima of energy for the collisionless case, computed by numerical integration of Eq. (25) with $\Lambda = 0$, are shown as circles in Fig. 10. These values are in agreement with the computer simulation results.

The collisional damping of the echo wave may be measured in terms of a collisional damping factor defined as

$$\kappa(t) = \ln \mid E_{3,\nu=0}^{\text{echo}}/E_{3,\nu}^{\text{echo}} \mid. \tag{28}$$

For the case of a collision frequency independent of velocity, the exponential $\exp(-\Lambda)$ may be taken out of the velocity integration in Eq. (25), whence

TABLE I

Comparison of the Collisional Damping Factor from Computer Simulation with Theoretical Values from O'Neil and from Ichikawa and Suzuki for the Case of a Velocity-Independent Collision Frequency

$\omega_p t$	κ_{sim}	κ_o	κ_{I-S}
31	0.47	2.44	0.60
33	0.67	2.50	0.77
35	1.0	2.54	1.12
37	1.47	2.55	1.61
39	2.10	2.56	2.24
41	2.58	2.56	3.02
43	2.71	2.56	3.97
45	2.66	2.58	5.08
47	2.62	2.61	6.37
49	2.65	2.67	7.85
51	2.54	2.82	9.52

Note. Parameters are the same as in Fig. 10.

TABLE II

Comparison of the Collisional Damping Factor from Computer Simulation with Theoretical Values from O'Neil and from Ichikawa and Suzuki for the Case of a Velocity-Dependent Collision Frequency

$\omega_p t$	κ_{sim}	κ_o	κ_{I-S}
31	0.18	0.88	0.25
33	0.11	0.91	0.31
35	0.32	0.96	0.37
37	0.66	1.11	0.65
39	1.41	1.62	1.47
41	1.67	1.66	1.84
43	1.46	1.33	2.01
45	1.22	1.05	2.00
47	1.08	0.92	2.16
49	1.02	0.92	2.45
51	0.91	0.95	2.81

Note. Parameters are the same as in Fig. 10.

$\kappa(t) = \Lambda(t)$. Values of this damping constant from the simulation results of Fig. 10 are compared in Table I with the analytical values from Eqs. (26) and (27). Note that for this case the coefficient D, given by Eq. (2), is $D = v_T^2$. We observe in Table I that the simulation results agree with O'Neil's result after the peak of the echo ($t > 40\omega_p^{-1}$) and agree approximately with the result of Ichikawa and Suzuki before the peak ($t < 40\omega_p^{-1}$). This appears to be consistent with the approximations made in these theories as indicated earlier.

For the case of a velocity dependent collision frequency, the analytical values of the collisional damping constant $\kappa(t)$ must be computed by numerical integration of Eq. (25), including the exponential $\exp(-\Lambda)$ in the velocity integration. In this case, the coefficient D, given by Eq. (2), is $D = 0.526 v_T^2$. Values of the damping constant from the simulation results of Fig. 10 are compared in Table II with the analytical values obtained from Eqs. (26) and (27). We observe again that the simulation results agree approximately with O'Neil's result after the peak of the echo ($t > 40\omega_p^{-1}$) and with the result of Ichikawa and Suzuki before the peak ($t < 40\omega_p^{-1}$). It is also interesting to observe that the collisional damping constant decreases with time after the peak, e.g., $\kappa\,(t = 41) = 1.67$ and $\kappa\,(t = 51) = 0.91$. This was a result predicted in O'Neil's theory for Coulomb collisions [14].

APPENDIX A: COLLISION OPERATOR

Consider the Fokker–Planck operator for electron–ion collisions [17],

$$\frac{1}{\Gamma}\left(\frac{\partial f}{\partial t}\right)_{\text{coll}} = -\frac{\partial}{\partial v^\alpha}\left(f\frac{\partial h}{\partial v^\alpha}\right) + \frac{1}{2}\frac{\partial^2}{\partial v^\alpha\,\partial v^\beta}\left(f\frac{\partial^2 g}{\partial v^\alpha\,\partial v^\beta}\right), \tag{A1}$$

where

$$\Gamma = (4\pi Z^2 e^4/m^2)\ln(9K^3T_e^3/4\pi n Z^2 e^6)^{1/2}.$$

In this equation f denotes the electron distribution function, v^α with $\alpha = 1, 2,$ and 3 denote the velocity components v_x, v_y, and v_z, n is the electron density, T_e is the electron temperature, K is Boltzmann's constant, Ze is the ion charge and $-e$ and m are the electron charge and mass. The functions h and g depend on the ion distribution function f_i, and ion mass m_i,

$$h(\mathbf{v}) = \frac{m + m_i}{m_i}\int \frac{f_i(\mathbf{v}')}{|\,\mathbf{v}' - \mathbf{v}\,|}\,d\mathbf{v}', \tag{A2}$$

$$g(\mathbf{v}) = \int |\,\mathbf{v}' - \mathbf{v}\,|\,f_i(\mathbf{v}')\,d\mathbf{v}'. \tag{A3}$$

Assuming stationary ions these functions reduce to $h = n/Zv$ and $g = nv/Z$, where $v = |\mathbf{v}|$. In the case of cylindrical symmetry about the x axis, integrating Eq. (A1) with respect to v_y and v_z gives

$$\left(\frac{\partial \bar{f}}{\partial t}\right)_{\text{coll}} = \frac{n\Gamma}{Z}\frac{\partial}{\partial v_x}\left\{v_x \int \frac{v_\perp}{(v_\perp^2 + v_x^2)^{3/2}} f\, dv_\perp + \frac{1}{2}\frac{\partial}{\partial v_x}\int \frac{v_\perp^3}{(v_\perp^2 + v_x^2)^{3/2}} f\, dv_\perp\right\}, \quad \text{(A4)}$$

where $\bar{f}(v_x) = \int (f/2\pi)\, dv_y\, dv_z$ is the one-dimensional velocity distribution function and $v_\perp = (v_y^2 + v_z^2)^{1/2}$ is the perpendicular velocity. This operator represents small-angle collisions between electrons and stationary ions. It yields a relaxation of anisotropies in the velocity distribution of electrons but no relaxation of their energy distribution. Computer simulations based on this collision operator would require a representation of the velocity distribution in the perpendicular direction as well as in the parallel direction. Since the perpendicular velocity $v_\perp$ cannot be eliminated by integration in the right member of Eq. (A4), a one-dimensional collision operator cannot be derived.

To carry out one-dimensional simulations, a model having some of the mathematical properties of Eq. (A4) must be chosen. In the present study we consider the operator

$$\left(\frac{\partial \bar{f}}{\partial t}\right)_{\text{coll}} = \frac{\partial}{\partial v_x}\left[\nu v_x \bar{f} + D\frac{\partial}{\partial v_x}(\nu \bar{f})\right], \quad \text{(A5)}$$

where

$$\nu = C/(2\langle v_x^2\rangle + v_x^2)^{3/2}, \quad \text{(A6)}$$

$C = nT/Z$, and D is a parameter to be chosen by energy considerations. The brackets $\langle ... \rangle$ denote an average over velocities, $\langle g\rangle = (1/n)\int g\bar{f}\, dv_x$, whence $\langle v_x^2\rangle$ is the mean square velocity. Note that the one-dimensional model (A5) retains two important properties of the original operator (A4): (1) It includes a first-order derivative term representing momentum loss due to collisions and a second-order derivative term which gives diffusion in velocity space, and (2) these effects fall off as v_x^{-3} for large velocities.

The evolution of the electron distribution function of a spatially homogeneous plasma, with the collisional operator (A5), is governed by

$$\frac{\partial f}{\partial t} - \frac{eE}{m}\frac{\partial f}{\partial v} = \frac{\partial}{\partial v}\left[\nu v f + D\frac{\partial}{\partial v}(\nu f)\right]. \quad \text{(A7)}$$

Here the notations have been simplified by writing f for the one-dimensional distribution function and v for the x component of the velocity. Integrating

Eq. (A7) over velocity yields $\partial n/\partial t = 0$, i.e., particle conservation, and taking the first and second moments gives

$$\frac{\partial \langle v \rangle}{\partial t} + \langle \nu v \rangle = -\frac{eE}{m} \tag{A8}$$

and

$$\frac{1}{2}\frac{\partial \langle v^2 \rangle}{\partial t} + \frac{eE}{m}\langle v \rangle = \langle v^2 \nu \rangle - D\langle \nu \rangle. \tag{A9}$$

The left member of Eq. (A9) represents the rate of change of the sum of the one-dimensional kinetic and potential energies per unit mass. In the present model we require this sum to be conserved, whence[1]

$$D = \langle v^2 \nu \rangle / \langle \nu \rangle. \tag{A10}$$

APPENDIX B: Derivation of Eq. (15)

At equilibrium, Eq. (11), with $f(v \to \infty) = 0$ yields

$$\nu v f + D\frac{\partial}{\partial v}(\nu f) = 0, \tag{B1}$$

which may be integrated to give

$$f(v) = \frac{f(0)\,\nu(0)}{\nu(v)}\, e^{-v^2/2D}. \tag{B2}$$

The normalization constant $f(0)$ and the parameter D are determined by the conditions

$$\int_{-\infty}^{+\infty} f\, dv = 1, \tag{B3}$$

$$\int_{-\infty}^{+\infty} v^2 f\, dv = \langle v^2 \rangle, \tag{B4}$$

[1] The original operator (A4) conserves the total kinetic energy but the one-dimensional kinetic energy, associated with the x direction, is not conserved due to energy transfer into the perpendicular direction. This energy transfer is neglected in the present one-dimensional model when D is computed from Eq. (A10), although this equation may be modified to take this effect into account.

where the mean square velocity $\langle v^2 \rangle$ is known since it remains constant during the approach to equilibrium. Substituting the collision frequency

$$\nu = C/(2\langle v^2 \rangle + v^2)^{3/2}$$

into (B2) and inserting the resulting expression into (B3) and (B4) yields

$$2^{1/2}\langle v^2 \rangle^{1/2} f(0) \int_{-\infty}^{+\infty} (1 + x^2)^{3/2} e^{-\alpha x^2} dx = 1 \tag{B5}$$

and

$$2^{3/2}\langle v^2 \rangle^{1/2} f(0) \int_{-\infty}^{+\infty} x^2(1 + x^2)^{3/2} e^{-\alpha x^2} dx = 1, \tag{B6}$$

where $\alpha = \langle v^2 \rangle / D$. The integrals in (B5) and (B6) may be expressed in terms of the modified Bessel functions of the second kind to give

$$f(0) = \frac{2^{1/2}}{\langle v^2 \rangle^{1/2}} e^{-\alpha/2} \left[K_0\left(\frac{\alpha}{2}\right) + \left(1 + \frac{1}{\alpha}\right) K_1\left(\frac{\alpha}{2}\right) \right]^{-1},$$

and

$$f(0) = \frac{\alpha}{(2\langle v^2 \rangle)^{1/2}} e^{-\alpha/2} \left[\frac{1}{2} K_0\left(\frac{\alpha}{2}\right) + \left(\frac{2}{\alpha} + \frac{1}{2}\right) K_1\left(\frac{\alpha}{2}\right) \right]^{-1}.$$

Solving these equations yields $\alpha = \langle v^2 \rangle / D = 1.76$ and $f(0) = 0.3537/\langle v^2 \rangle^{1/2}$. Substitution of these values into Eq. (B2) and renormalization to the density n yields Eq. (15).

Acknowledgments

This research is supported jointly by the U.S. Atomic Energy Commission under contract AT(11-1)-2200 and the Office of Naval Research under contract N00014-67-A-0356-0026 and has been carried out in cooperation with the Lawrence Livermore Laboratory.

References

1. W. L. Kruer, P. K. Kaw, J. M. Dawson, and C. Oberman, *Phys. Rev. Lett.* **24** (1970), 987; W. L. Kruer and J. M. Dawson, *Phys. Fluids* **15** (1972), 446; J. S. DeGroot and J. I. Katz, *Phys. Fluids* **16** (1973), 401.
2. J. Denavit, "Collisional Effects on Electron Heating Due to Parametric Instabilities" 4th Anomalous Absorption Conference, Lawrence Livermore Laboratory, April 8–10, 1974, to be published.
3. J. Denavit, *J. Computational Phys.* **9** (1972), 75.

4. A. LENARD AND I. B. BERNSTEIN, *Phys. Rev.* **112** (1958), 1456.
5. V. E. ZAKHAROV AND V. I. KARPMAN, *Ž. Èksper. Teoret. Fiz.* **43** (1962), 490 [*Soviet Physics JETP* **16** (1963), 351].
6. J. DENAVIT, B. W. DOYLE, AND R. H. HIRSH, *Phys. Fluids* **11** (1968), 2241.
7. F. C. GRANT AND R. FEIX, *Phys. Fluids* **10** (1967), 698; T. ARMSTRONG AND D. MONTGOMERY, *J. Plasma Phys.* **1** (1967), 425; G. JOYCE, G. KNORR, AND H. MEIER, *J. Computational Phys.* **8** (1971), 53.
8. J. KILLEEN AND K. D. MARX, "Methods in Computational Physics," Vol. 9, pp. 422–489, Academic Press, New York, 1970.
9. W. P. GULA AND C. K. CHU, *Phys. Fluids* **16** (1973), 1135.
10. R. SHANNY, J. M. DAWSON, AND J. M. GREENE, *Phys. Fluids* **10** (1967), 1281; **12** (1969), 2227.
11. J. S. DEGROOT, private communication.
12. T. M. O'NEIL AND R. W. GOULD, *Phys. Fluids* **11** (1968), 134.
13. C. H. SU AND C. OBERMAN, *Phys. Rev. Lett.* **20** (1968), 427.
14. T. M. O'NEIL, *Phys. Fluids* **11** (1968), 2420.
15. Y. H. ICHIKAWA AND T. SUZUKI, *Progr. Theoret. Phys.* **41** (1969), 313.
16. J. U. BRACKBILL, *Numerical simulation of plasma wave echoes with the distribution pushing algorithm*, Ph.D. Thesis, University of Wisconsin, 1971.
17. M. N. ROSENBLUTH, W. M. MACDONALD, AND D. L. JUDD, *Phys. Rev.* **107** (1957), 1.